

Experimental study on the use of compound alkaline materials to solidify lake sediments

Hongdan Yu, Kai Zhang, Haifeng Lu, and Qingzhao Zhang

- Due to its poor mechanical properties and contamination, sediment from dredging and lakeside construction projects is difficult to use directly in resource applications.
- Orthogonal tests, compressive strength measurements, and X-ray diffraction spectrum and scanning electron microscope analyses were used to investigate the solidification effects of three types of alkaline materials used alone or in combination with lake sediment: straw ash, calcium lime, and sodium silicate.
- Sediment solidification was aided by suitably alkaline conditions and large quantities of active silicon-calcium components, and the microstructures of the cured samples were more compact and had improved mechanical properties.

Sediment waste is a problem associated with dredging and waterside construction projects.¹⁻³ Sediment in lakes and rivers contains clay and organic matter, and it tends to have high water content and poor mechanical properties. It can also be contaminated with toxic and harmful substances such as pathogens and heavy metals. Given these characteristics, sediment from rivers and lakes usually cannot be directly used for large-scale resource applications.^{4,5} As a result, large amounts of sediment from dredging and construction projects are discarded, which not only adds to landfills but also can damage marine and terrestrial environments. Furthermore, improper disposal of sediment from dredging and construction projects can cause safety hazards. Therefore, there is an urgent need to develop safe methods to manage sediment disposal and resource use.⁶ One promising option is to treat sediment with materials that will induce alkali-activated reactions to solidify the sediment and create a stronger, more useful composite. To expand the body of knowledge on this option, a comprehensive analysis of the effects of selected types of solidifying materials on lake sediment was conducted. Based on our findings, an economical and scientific method to treat this type of sediment is proposed.

The sediment treatment experiments described in this paper draw from past research by Glukhovskiy⁷ and others,⁸⁻¹³ who found that in an alkali-activated reaction, the raw materials rich in silicon and aluminum elements undergo a process of dissolution, diffusion, polymerization, and curing, ultimately forming a cementitious material with good mechanical prop-

erties and corrosion resistance. This material is also known as geopolimer.

There is a wide range of raw materials that can be the sources for geopolimers. According to their elemental composition, these materials can be divided into two categories: high-calcium, low-aluminum raw materials, represented by slag and coal gangue, and high-aluminum, low-calcium raw materials, represented by metakaolin and activated sediment.¹⁴ Sediment is characterized by calcium deficiency, and sediment is mostly an inert component formed by chemical deposition. When sediment is solidified by alkali-activated reaction, its macro-mechanical properties are usually poor.¹⁵

Traditional sediment treatment methods involve incineration and solidification by drying. Such methods are inefficient and consume high amounts of energy. However, the development of alkali-activated materials has inspired new ideas for soil reinforcement.¹⁶ Researchers^{17,18} have proposed the use of fly ash or slag mixed with sodium silicate to prepare geopolimer slurry for the treatment of muddy clay, which has achieved good reinforcement effect. In this kind of treatment method, the soil is only used as the reinforced object and forms a composite material with the geopolimer, thereby improving the overall mechanical properties and not directly participating in the curing reaction.

Direct solidification of sediment by alkali-activated reaction is being explored as a method for sediment disposal. Alkali-activated reactions are used to strengthen and solidify river and lake sediment and fixate pollutants in the sediment. Lu et al.¹⁹ used alkali-activated reaction and thermal activation to synergistically treat sediment solid waste, and the obtained geopolimer sample had a 7-day compressive strength of

8.93 MPa (1300 psi) and a 28-day compressive strength of 16.37 MPa (2374 psi). Compared with the method of alkali-activated reaction only, the compressive strength of the sample was improved by a maximum of 1587%. When Kong et al.²⁰ used magnesium oxide (MgO) and industrial waste residue in combination to solidify the sediment, the researchers found that the 28-day maximum compressive strength could reach 4.29 MPa (622 psi), saving about 50% of the cost of calcination activation, which meant that the solidification treatment of sediment achieved meaningful economic and environmental benefits. In terms of activators, previous research has mainly concluded that the preparation of geopolimers by composite activators can use the chemical reaction between activators to generate intermediate products to promote the polymerization reaction²¹ and appropriate composite activators can be used to adjust the relevant properties of the prepared geopolimer to meet the intended uses of the material.²²

In previous research, most of the schemes for solidifying sediment based on the principle of alkali-activated reaction have used alkali activators such as sodium silicate or sodium hydroxide as a single curing material to treat sediment. These schemes usually have the disadvantages of a poor sediment solidification effect, a complex solidification process, and high costs.^{23,24} To address these problems, this study investigated the use of low-cost straw ash solid waste, calcium lime (as an alkaline calcium source additive), and traditional sodium silicate as curing materials. The orthogonal experimental design method was used to study the solidification effect of these different types of alkaline materials used alone or in combination with lake sediment, and to analyze the mechanism of sediment solidification by compound-doped materials, so as to find a scientifically sound, economical, and reliable method of sediment solidification.

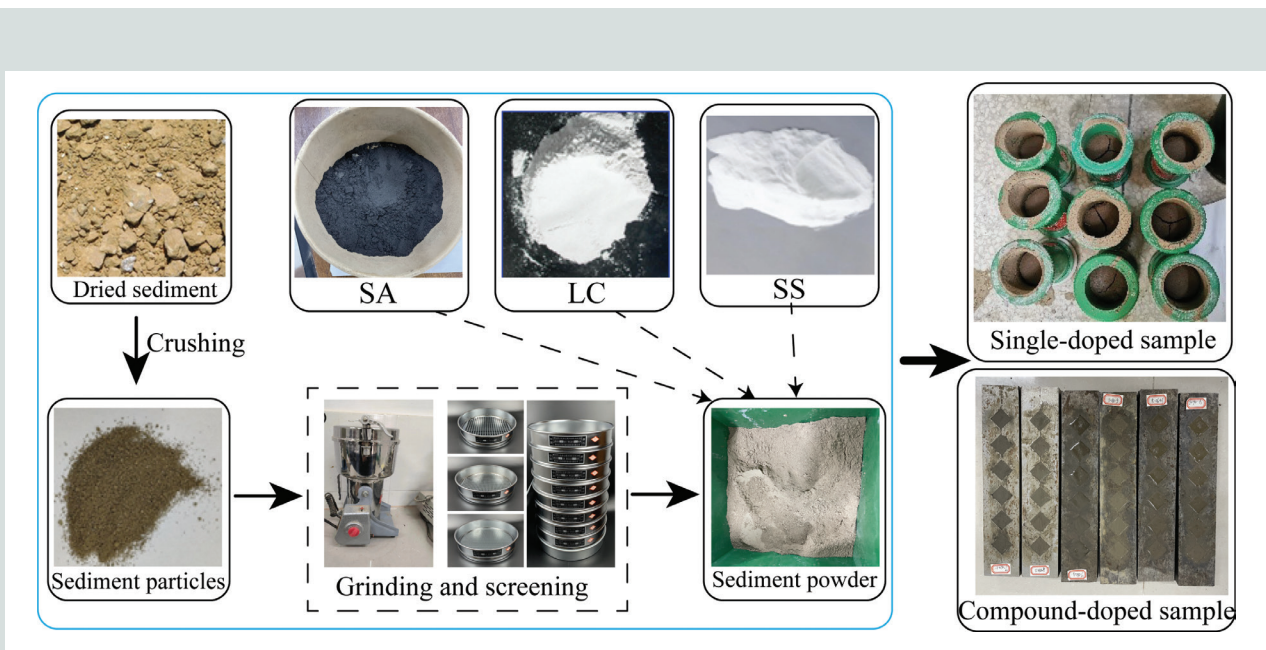


Figure 1. Sediment treatment and sample preparation process. Note: CL = calcium lime; SA = straw ash; SS = sodium silicate.

Experimental materials

Sediment

Dredging and waterside construction projects produce mixed sedimentary materials mainly composed of clay and organic matter.²⁵ The sediment used in this study came from the Nanhu Lake in Wuhan, China. This lake has light organic contamination and low amounts of organic matter. The original sediment after desilting was naturally condensed with a large block size (Fig. 1). To prepare it for study, the sediment was crushed with a hammer, ground with a vibrating mill, and finally sieved through a 200-mesh (0.074 mm [0.0029 in.]) screen. Figure 1 shows the sediment before crushing, after crushing, and after grinding and sieving. In the photos, the sediment color varies across the stages. These color changes are related to variations in the light and the particle sizes; they do not represent chemical changes in the samples.

An X-ray fluorescence (XRF) spectrometer was used to analyze the chemical composition of the lake sediment. The results of this analysis include the following with the values representing % by weight of each element (in the form of oxides of each element):

- SiO₂: 49.74%
- Al₂O₃: 22.19%
- Fe₂O₃: 7.98%
- K₂O: 2.37%
- MgO: 1.84%
- CaO: 1.76%
- TiO₂: 1.42%
- others: 1.75%
- loss on ignition (LOI): 10.95%

The LOI is the percentage of mass of the raw material that is lost when a sample is dried in the range of 100°C to 105°C (212°F to 221°F) and then burned at 1000°C until the weight was constant. The LOI of raw materials can represent the amount of gas released by physical evaporation or chemical decomposition of raw materials after heating. The chemical composition of the sediment in this investigation is similar to that of fly ash and metakaolin,²⁶ which belong to the category of low-calcium solid waste. The XRF results showed that the sediment contained large amounts of aluminum and silicon, thereby meeting the requirements for geopolymer preparation.²⁷

Straw ash

Straw ash is the residue of plants after burning. It contains all

the minerals in the plants, with potassium accounting for the highest percentage, generally 6% to 15%. The straw ash used in this study was a black powder solid. Before use, the straw ash was sieved through a 200-mesh (0.074 mm [0.0029 in.]) sieve. The XRF testing determined the chemical composition of the straw ash to be following with the values representing % by weight of each element (in the form of oxides of each element):

- SiO₂: 27.94%
- K₂O: 14.06%
- CaO: 11.39%
- MgO: 8.50%
- Cl: 3.43%
- Al₂O₃: 3.09%
- P₂O₅: 2.91%
- others: 2.97%
- LOI: 25.71%

Calcium lime

Calcium lime is a commonly used building material.²⁸ It can react with water to form a strong alkaline (calcium hydroxide) and release heat. The type of calcium lime used in this study is an analytically pure, white powder solid.

Sodium silicate

Sodium silicate (Na₂O·*n*SiO₂) is a white solid that is soluble in water. Its aqueous solution is a colorless and transparent viscous liquid, often called “water glass,” which is widely used in the construction industry.

The modulus *n* is an important parameter of sodium silicate. The smaller the *n* is, the greater the pH value of the sodium silicate solution is. The modulus *n* can be reduced by adding sodium hydroxide.²⁹ In this study, industrial-grade, powdery instant sodium silicate with a reduced modulus of 1.5 was used.

Water

Ordinary tap water from Wuhan was used in the experiment.

Mixture design and sample preparation

Single-doped solidified sediment testing

To study the solidification effects of selected types of solidifying materials on the sediment, single-doped testing was first conducted on samples of the sediment solidified with straw

ash, calcium lime, or sodium silicate. **Table 1** presents the designs for these tests.

The unconfined compressive strengths of samples with different proportions (mass ratio of solidifying material to dried sediment) and different curing ages (three days versus seven days) were used as the indexes to study the effect of each solidifying material on the compressive strength of the sediment. In these tests, the water-to-solid ratio (the ratio of water by mass to the sum of the mass for all other materials) was 0.5.

After mixing the raw materials according to the proportions in Table 1, the slurry mixture was poured into standard cylindrical molds with an inner diameter of 50 mm (2 in.) and a height of 100 mm (4 in.), where it was fully vibrated and compacted (Fig. 1). The samples were unmolded after curing for 24 hours in an indoor environment and then continued to cure to the specified age.

Orthogonal testing of the compound-doped solidified sediment

According to the principle of alkali-activated solidification of sediment, the combined use of different types of solidifying material may promote the compressive strength of sediment. To avoid unnecessary intervention combinations, the number of test combinations used to assess the influence of multiple factors on the mechanical properties of solidified sediment should be minimized.²⁹ In this investigation, the orthogonal experimental design method was used to design the material mixture proportions and prepare samples. From the content of solidifying material, the straw ash to lake sediment content, the calcium lime to lake sediment content, and the sodium silicate ($\text{Na}_2\text{O}\cdot n\text{SiO}_2$) to lake sediment content were selected as three factors of orthogonal design. The setting range of each factor is 0.05 to 0.25, and the step size is increased

by 0.1. The factor levels of the orthogonal test included the following:

- level 1: 5% content of each added material (straw ash, calcium lime, and sodium silicate)
- level 2: 15% content of each added material (straw ash, calcium lime, and sodium silicate)
- level 3: 25% content of each added material (straw ash, calcium lime, and sodium silicate)

The sample preparation included three steps: preparation of the compound curing-material solution, pouring, and curing (Fig. 1). Following the mixture proportions in **Table 2**, the solidifying materials and water were mixed thoroughly to create a compound solution, and then the sediment was mixed with the compound solution and stirred for three minutes. Next, the stirred slurry was poured into a standard abrasive tool measuring $20 \times 20 \times 20$ mm (0.8 in.), fully vibrated, and compacted. The samples were unmolded after curing for 24 hours at room temperature, and then curing continued to the specified age. The curing temperature was $20^\circ\text{C} \pm 2^\circ\text{C}$ ($68^\circ\text{F} \pm 4^\circ\text{F}$), and the relative humidity was about 65% to 70%.

Testing and characterization methods

Unconfined compressive strength tests

Cylindrical samples 50 mm (2 in.) in diameter and 100 mm (4 in.) long were prepared by static pressure method, with three parallel samples in each group. After the samples reached their curing ages (three or seven days), their compressive strength was tested with a strain-controlled unconfined compressive strength testing instrument. The load interval was set to 1 mm/min (0.04 in./min), and the maximum range of the instrument was 10 kN (2.2 kip).

Table 1. Single-doped test design

Solidifying material	Solidifying material content		Lake sediment, g	Water, g	Curing age, days
	%	g			
Straw ash	5	5	100	52.5	3, 7
	10	10		55	
	15	15		57.5	
Calcium lime	5	5		52.5	
	10	10		55	
	15	15		57.5	
Sodium silicate	5	5		52.5	
	10	10		55	
	15	15		57.5	

Note: 1 g = 0.0353 oz

Table 2. Orthogonal experiments for compound-doped samples

Mixture	Content of solidifying materials, %			Content of solidifying materials, g			Lake sediment, g	Water, g	Compressive strength, MPa*	
	Straw ash	Calcium lime	Sodium silicate	Straw ash	Calcium lime	Sodium silicate			Three days	Seven days
SM1-A1B1C1	5	5	5	5	5	5	100	57.5	1.11	1.15
SM2-A1B2C2	5	15	15	5	15	15	100	67.5	2.76	3.80
SM3-A1B3C3	5	25	25	5	25	25	100	77.5	4.89	7.18
SM4-A2B1C2	15	5	15	15	5	15	100	67.5	1.06	1.88
SM5-A2B2C3	15	15	25	15	15	25	100	77.5	1.95	3.00
SM6-A2B3C1	15	25	5	15	25	5	100	72.5	1.39	2.34
SM7-A3B1C3	25	5	25	25	5	25	100	77.5	0.43	1.77
SM8-A3B2C1	25	15	5	25	15	5	100	72.5	2.40	2.41
SM9-A3B3C2	25	25	15	25	25	15	100	82.5	2.87	5.22

Note: 1 MPa = 0.145 ksi.

*Calculated as the average compressive strength of three samples.

Uniaxial compressive strength tests

The uniaxial compressive strength test of the compound material–solidified sediment was conducted in the uniaxial compression mode of a stability testing device (Fig. 1). The maximum range of the instrument was 50 kN (11 kip), the loading rate was controlled to 1 mm/min (0.04 in./min), and sample compressive strengths were tested at 3 and 7 days. Three parallel 50 × 50 × 50 mm (2 × 2 × 2 in.) cube samples were prepared in each group. According to the test method standard for the physical and mechanical properties of concrete, the cubic compressive strength R_c of the sample is defined as the stress when the sample is destroyed.

X-ray diffraction test

An X-ray diffractometer was used to analyze the phase of the samples with a scanning range of 20 to 60 degrees. The glass tube anode type of the machine was copper, the test speed was set to 5 degrees per minute, and the step length was 0.02 degrees.

Scanning electron microscope

Investigators used a general-purpose, thermal-type scanning electron microscope to observe the samples. The test voltage was 5 kV, and the SE (secondary electron signal imaging) mode was adopted.

Results and discussion

Sediment properties

The lake sediment in this study was prone to softening and swelling in water and shrinking and cracking during water

loss. Such effects occurred because the sediment’s internal structure was changed by reactions between clay minerals and water. For example, illite, which constituted up to 20% of the lake sediment, can swell by as much as 50% when exposed to water.²⁷

In this study, the sediment was used as the raw material. After it was crushed, it was mixed with water to create a slurry with a water-to-solids ratio of 0.5. The slurry had good fluidity, but the sample shrank and cracked substantially during the curing process (Fig. 2), and here demolding does not produce a complete specimen and the specimen compressive strength can be approximated as 0.

We conducted experiments and found that when the ratio of water to solids was reduced below 0.5, it was more difficult to mix the slurry due to the hydrophilicity of the clay minerals in the sediment. In the natural state, clay mineral will absorb



Figure 2. Shrinkage and cracking of dried lake sediments.

water and swell.³⁰ In addition, the compressive strength of the sample dropped significantly after it was exposed to water. Thus, the lake sediment had poor mechanical properties, and could not be used before it underwent a series of treatments.

The mineral composition of the lake sediment was analyzed by X-ray diffraction (XRD). The various peaks of the XRD spectrum characterize the different crystal structures of illite, kaolinite, quartz, chlorite, microcline intermediate, and albite (Fig. 3). A similar peak has been found in the XRD of metakaolin, a geopolymer precursor.^{31,32} Based on the XRF and XRD analyses of the lake sediment, it was found that although there was a large amount of silicon in the lake sediment, most of it was in the form of crystals, whereas the content of amorphous silicon, a precursor of geopolymer reaction,^{33–35} was relatively low. This property of illite to expand by about 50%

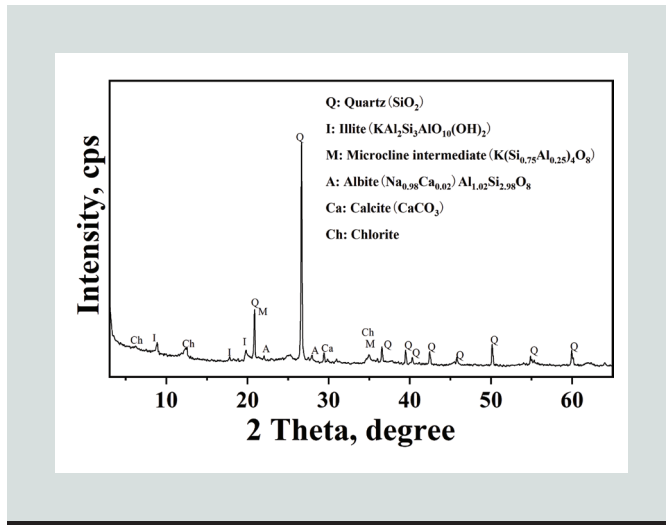


Figure 3. Results of the X-ray diffraction spectrum analysis of the lake sediment. Note: θ = the diffraction half angle.

when it absorbs water explains why the lake sediment shrank when water was lost.³⁶

Single-doped sample analyses

Straw ash-solidified sediment The straw ash used in this investigation is light, more than 90% of its components are water-soluble substances, and its aqueous solution is alkaline. The alkalinity of the straw ash is mainly provided by potassium oxide (K_2O), and the pH value of the saturated aqueous solution of straw ash is about 12. The straw ash also contains a fair amount of silicon dioxide (SiO_2), which has the potential to participate in alkali-activated reactions.

The addition of too much straw ash to a sample will substantially increase water demand, leading to notable cracking during curing. In this investigation, samples with three different amounts of straw ash (5%, 10%, and 15%) were tested.

Figure 4 shows the 5%, 10%, and 15% straw ash-solidified samples in compression failure. During the testing, the samples exhibited considerable shrinkage and cracking. The failure modes of the samples were similar, with most caused by tensile failure.

Figure 5 plots the average compressive strengths of each sample type. The highest seven-day compressive strength for a straw ash single-doped sample was 0.32 MPa (46 psi), and the lowest seven-day compressive strength was 0.18 MPa (26 psi). The compressive strengths of the samples decreased as the straw ash content increased. This finding may be due to undissolved straw ash filling in the solidified sediment, leading to the formation of micro-cracks, which weaken the sample compressive strength. The samples were not high in compressive strength, but the addition of straw ash did make them somewhat stronger than the untreated sediment.

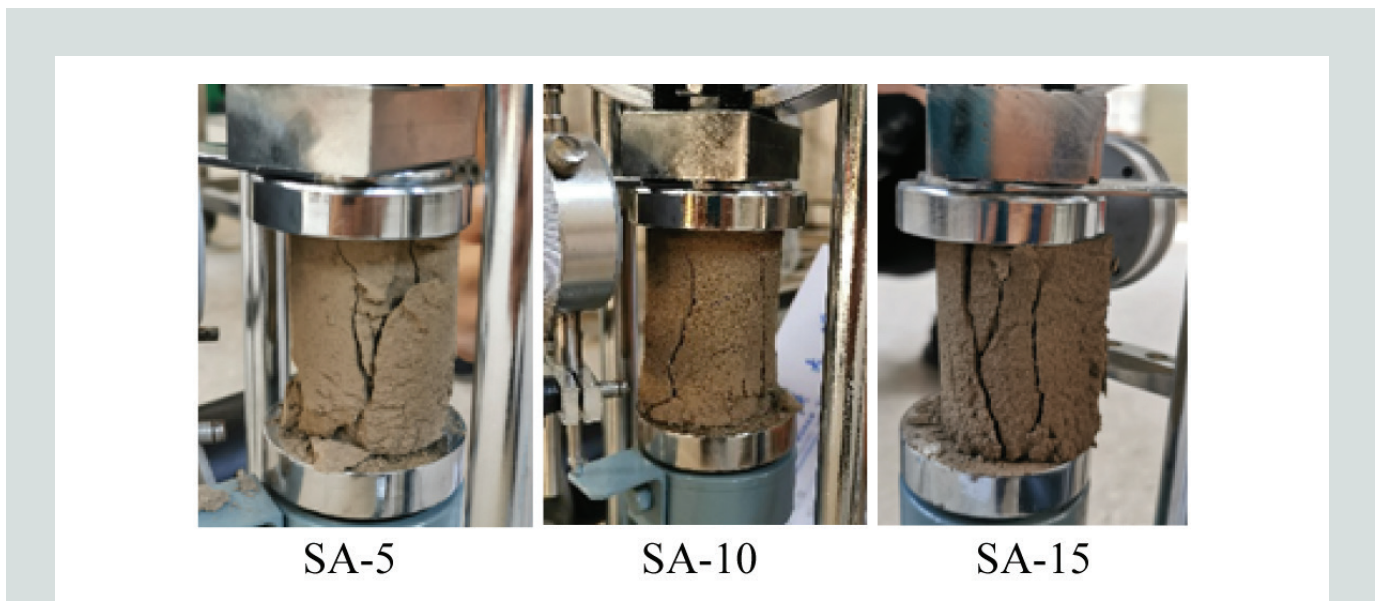


Figure 4. Failure modes of single-doped samples with percentage of straw ash content by weight. Note: SA-5 = 5% straw ash content by weight; SA-10 = 10% straw ash content by weight; SA-15 = 15% straw ash content by weight.

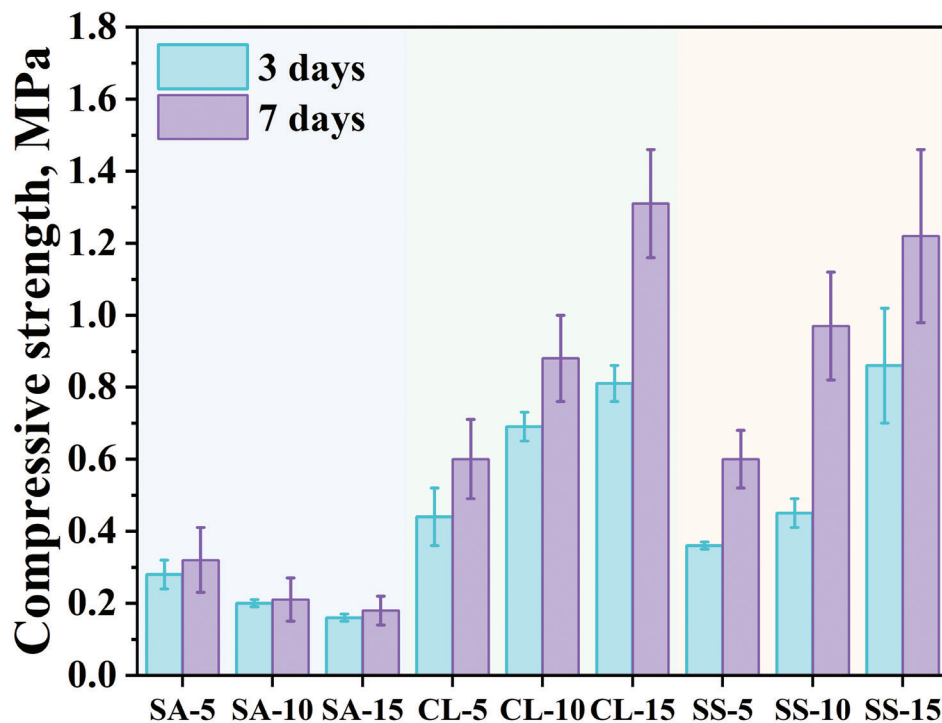


Figure 5. Average compressive strengths of the single-doped samples. Note: CL-5 = 5% calcium lime content by weight; CL-10 = 10% calcium lime content by weight; CL-15 = 15% calcium lime content by weight; SA-5 = 5% straw ash content by weight; SA-10 = 10% straw ash content by weight; SA-15 = 15% straw ash content by weight; SS-5 = 5% sodium silicate content by weight; SS-10 = 10% sodium silicate content by weight; SS-15 = 15% sodium silicate content by weight. 1 MPa = 0.145 ksi.

Calcium lime–solidified sediment Figure 5 plots the compressive strengths of the samples with 5%, 10%, and 15% calcium lime content.

The lowest and highest compressive strengths for the calcium lime single-doped samples cured for three days were 0.44 and 0.81 MPa (64 and 120 psi), respectively. When cured for seven days, the samples had compressive strengths ranging from 0.6 to 1.31 MPa (87 to 190 psi). Because calcium oxide could generate a strong alkaline solution with water, it provided favorable conditions for the sediment to participate in an alkali-activated reaction. At the same time, the by-product calcium hydroxide could react with carbon dioxide in the air to form calcium carbonate with high compressive strength, which also contributed to the improvement of the overall sample compressive strength. The results indicate that the compressive strength of the sample increased as calcium lime content increased (Fig. 5).

Sodium silicate–solidified sediment After curing for seven days, the samples were smooth, compact, and crack free, without the appearance of alkali precipitation.

Figure 5 plots the compressive strengths of the samples with 5%, 10%, and 15% sodium silicate content. The compressive strength of samples that had been cured for 3 days ranged from 0.36 to 0.86 MPa (52 to 125 psi). When cured for seven

days, samples ranged in compressive strength from 0.60 to 1.22 MPa (87 to 177 psi). There was a positive correlation between the compressive strength of the samples and the content of sodium silicate.

Analysis of the compound-doped solidified sediment samples

Uniaxial compressive strength In this part of the study, investigators prepared nine groups of samples by the orthogonal experimental design method, which can quantify the order of contribution of three influencing factors to compressive strength. At the same time that the samples were prepared, the solidification effects of the combined solidifying materials on the sediment were observed.

For each group of experiments, six samples were prepared. Table 2 presents the results of the uniaxial compression testing for the nine experimental groups, with data on the uniaxial compressive strengths for each group representing the average compressive strength of three samples at three or seven days of curing.

Figure 6 shows the apparent morphology of the compound-doped samples cured for three days. As the calcium lime and sodium silicate content increased, the samples were smoother and denser, and the phenomenon of deblocking on

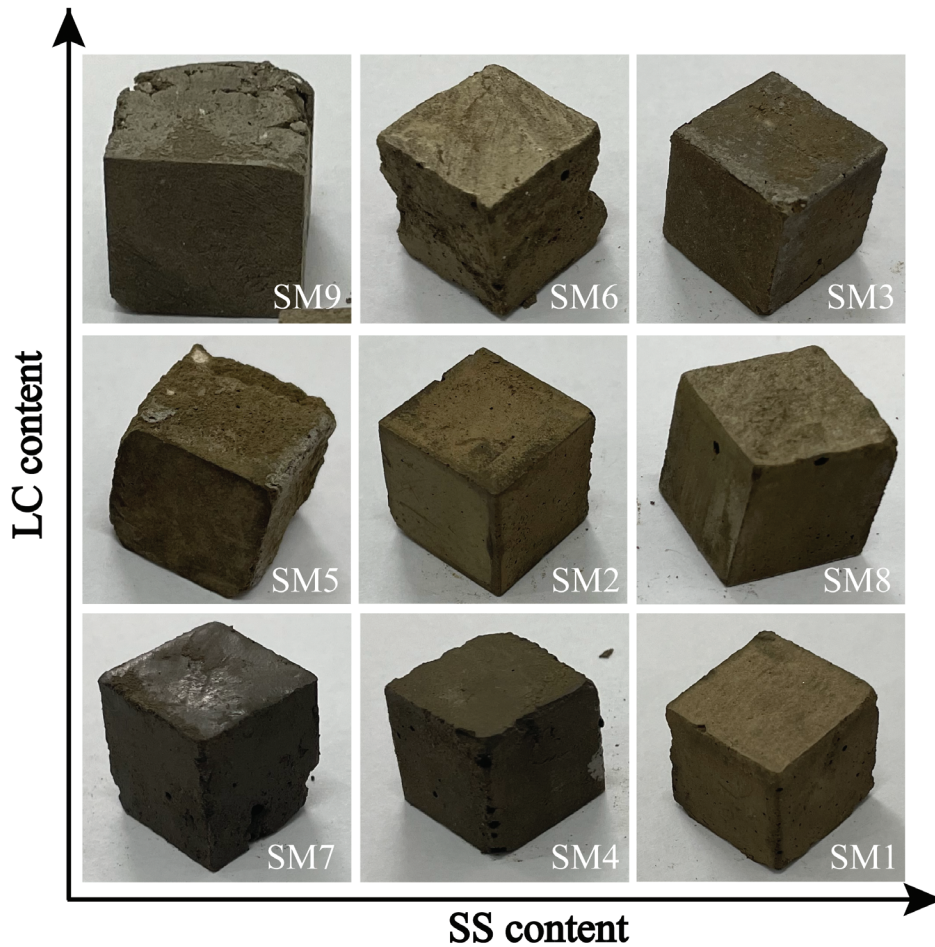


Figure 6. The apparent morphologies of the nine types of compound-doped samples after three days of curing. Note: CL = calcium lime; SS = sodium silicate.

the surface was reduced. The cohesion of the sample itself also increased, with the apparent pores reduced accordingly. Compared with the single-doped samples, the compound-doped samples experienced shear failure, and the degree of fragmentation in the compound-doped samples was also low.

Figure 7 shows a histogram of the average uniaxial compressive strengths of the nine types of compound-doped samples. At three days of curing, the compressive strengths of samples in the nine compound-doped groups ranged from 0.43 to 4.89 MPa (62 to 709 psi). When these values are compared with the compressive strengths of the single-doped samples at three days of curing (0.16 to 0.28 MPa [23 to 41 psi] for straw ash, 0.44 to 0.81 MPa [64 to 120 psi] for calcium lime, and 0.36 to 0.86 MPa [52 to 125 psi] for sodium silicate), it is clear that alkali-activated modification had a significant effect on the physical and mechanical properties of the compound-doped samples. Moreover, at seven days of curing, the compressive strengths in each group of compound-doped samples were further improved, with the minimum compressive strength being greater than 1 MPa (145 psi) and the maximum compressive strength reaching 7.18 MPa (1040 psi).

Range analysis of the uniaxial compressive strength

Due to the comprehensive comparability of the orthogonal test, in the range analysis, T_{Aj} represents the sum of the data of all levels under the factor A, and the data changes of \bar{T}_{Aj} (the average of the j -level data of the factor A) can be generally regarded as being caused by the different levels of the factor A. The range R_A (the difference between the maximum and minimum values of \bar{T}_{Aj}) can be regarded as the approximated degree of change in the whole test caused by the level change of factor A. Thus, the primary and secondary factors of the test can be compared intuitively, and the optimal level of collocation can be found through fewer test groups.³⁷

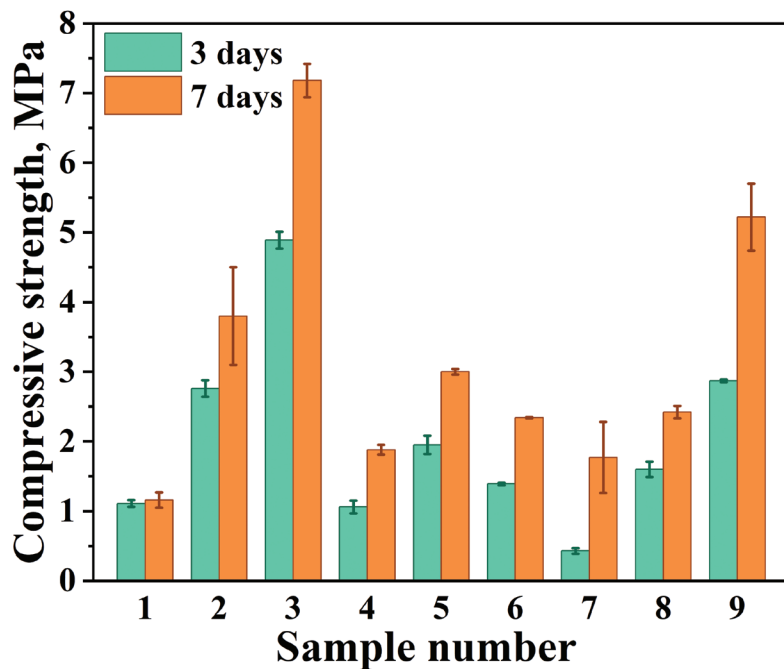
Table 3 presents the range analysis of the compressive strengths of the compound material–solidified samples at three and seven days of curing. The order of sensitivity of the compressive strength to various factors in the mixture is as follows:

- For three-day compressive strength, calcium lime content > straw ash content > sodium silicate content

Table 3. Range analysis for compressive strengths of compound-doped samples

Factors	Three-day compressive strength			Seven-day compressive strength		
	Straw ash	Calcium lime	Sodium silicate	Straw ash	Calcium lime	Sodium silicate
T_{i1}	8.758	2.595	4.100	12.13	4.79	5.90
T_{i2}	4.405	6.313	6.690	7.21	9.21	10.89
T_{i3}	4.890	9.145	7.263	9.40	14.74	11.95
\bar{T}_{i1}	2.919	0.865	1.367	4.04	1.60	1.97
\bar{T}_{i2}	1.468	2.104	2.230	2.40	3.07	3.63
\bar{T}_{i3}	1.630	3.048	2.421	3.13	4.91	3.98
R_i	1.451	2.183	1.054	1.64	3.31	2.02

Note: R_i = range (difference between the maximum and minimum values of \bar{T}_{A_i}); T_{i1} = sum of the data of levels 1 under the factor i (A, B, or C); T_{i2} = sum of the data of levels 2 under the factor i (A, B, or C); T_{i3} = represents the sum of the data of levels 3 under the factor i (A, B, or C); \bar{T}_{i1} = mean value (numerically equal to T_{i1} divided by the levels number); \bar{T}_{i2} = mean value (numerically equal to T_{i2} divided by the levels number); \bar{T}_{i3} = mean value (numerically equal to T_{i3} divided by the levels number).

**Figure 7.** Average three- and seven-day uniaxial compression strengths for the nine types of compound-doped samples. Note: 1 MPa = 0.145 ksi.

- For seven-day compressive strength, calcium lime content > sodium silicate content > straw ash content

Using data from Table 3, **Figure 8** illustrates the trends for the influence of various factors on the compressive strength of the compound-doped samples. From these trends, it can be determined that the compressive strength of the solidified sediment can reach the maximum value when the straw ash content is 5%, the calcium lime content is 25%, and the sodium silicate content is 25%.

Analysis of the trends for each factor's influence on the compressive strength of the sample indicates that the internal mechanism is as follows:

- A small amount of straw ash can improve the pH value of the reaction environment to an extent, promote the sediment's participation in the alkali-activated reaction, and improve the compressive strength of the samples. However, given the weak alkalinity provided by straw ash, some weak impurities that do not participate in the reaction are

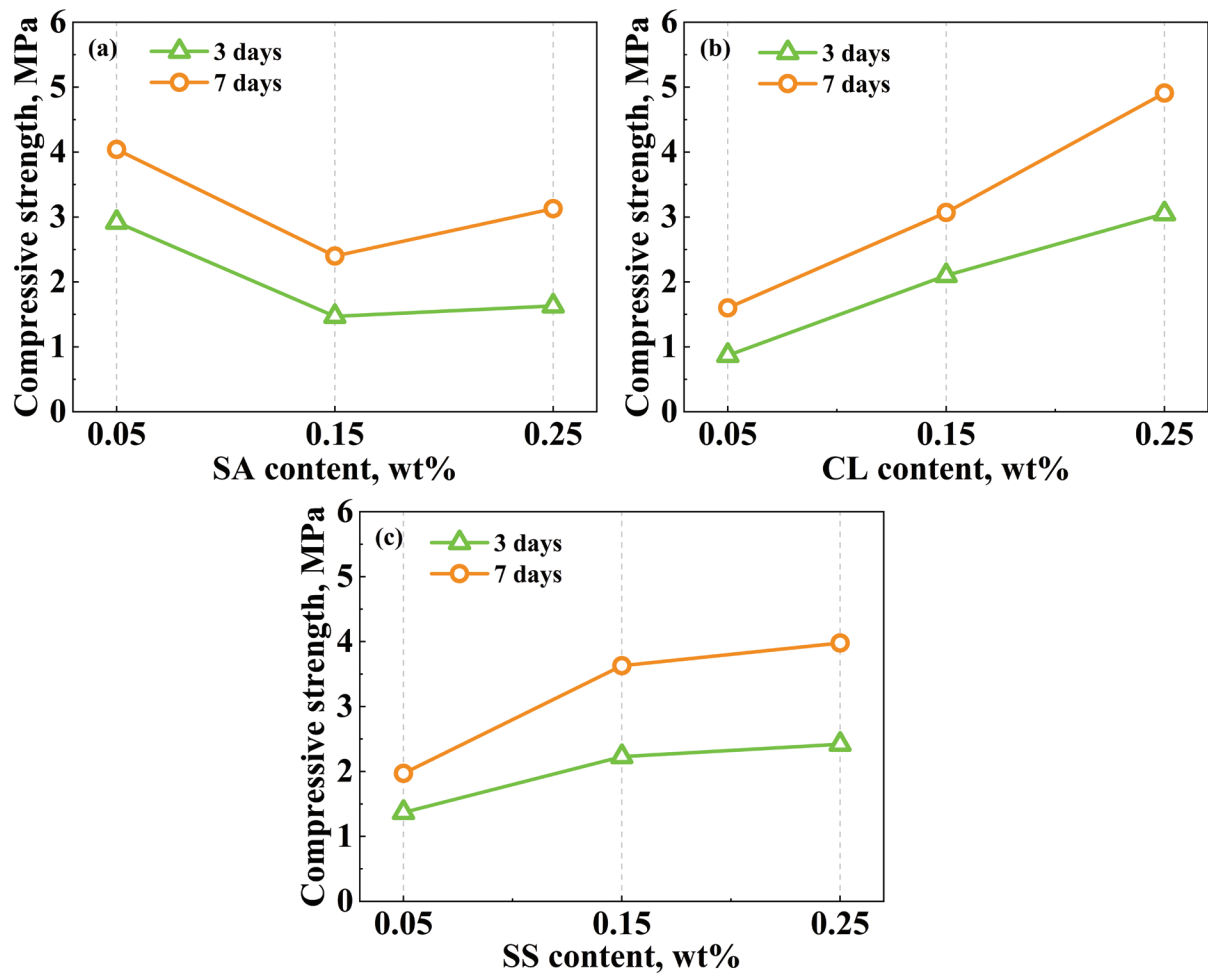


Figure 8. Influence trends for each factor on the compressive strength of the compound-doped samples. Note: 1 MPa = 0.145 ksi.

introduced. Therefore, a high proportion of straw ash will weaken the compressive strength of the sample.³⁸

- The lake sediment was low in calcium, and the input of calcium from the calcium lime additive supplemented the early compressive strength of samples, with the compressive strength increasing linearly as the calcium lime content increased. This finding is mainly attributed to the existence of a large number of calcium source precursors in the reaction system, which effectively accelerates the hydration rate of the geopolymer system.^{39,40}
- The sodium silicate content reflects the concentration of the sodium silicate ($\text{Na}_2\text{O} \cdot n\text{SiO}_2$) in the solution. Figure 8 shows that a higher sodium silicate content does not necessarily increase the compressive strength of the sample. The amount of active silicon in the sediment is low. The addition of the silicate alkali activator can provide several silicon components for the reaction, and the geopolymer reaction was promoted by controlling the relative coordination of silicon and aluminum leaching rate.²⁹

Analysis of variance for uniaxial compressive strength

Range analysis can identify the primary and secondary sorting of each influencing factor to clarify the main factors affecting the compressive strength of the solidified sediment samples. However, in an orthogonal test, the change in the compressive strength index may be attributed to either the change in the factor level or random error of the test. Because it cannot be determined from range analysis how much influence to attribute to the factors versus random error, we need to use analysis of variance to calculate the difference between the fluctuation of the compressive strength index caused by each factor and the fluctuation caused by random error. From this analysis, we can thus determine the significance of each factor's influence on the compressive strength index.

The compressive strength results of the solidified sediment samples at three and seven days of curing were analyzed by analysis of variance. **Table 4** presents the statistical indexes. The larger the *F*-value in the table is, the greater the influence of the corresponding factors is on the compressive strength of

Table 4. Analysis of variance for compressive strengths of compound-doped samples

Factors	Three-day compressive strength				Seven-day compressive strength			
	Sum of squares	Degree of freedom	Mean square sum	<i>F</i>	Sum of squares	Degree of freedom	Mean square sum	<i>F</i>
Straw ash	3.79	2	1.90	2.57	4.04	2	2.02	1.88
Calcium lime	7.19	2	3.60	4.88	16.54	2	8.27	7.71
Sodium silicate	1.89	2	0.95	1.28	6.95	2	3.48	3.24
Experimental error	1.47	2	0.74	n/a	2.15	2	1.07	n/a
Total data volatility	14.35	8.00	$F_{(3,3)0.10} = 5.36$		29.68	8.00	$F_{(3,3)0.10} = 5.36$	

Note: *F* = *F*-test value; $F_{(3,3)0.10}$ = *F*-critical value where there is at least a 90% probability that two sets of data (both 3 degrees of freedom) have a significant difference; n/a = not applicable.

the sample. The relative degree of influence of each factor on the compressive strength of the samples is as follows:

- For three-day compressive strength, calcium lime content > straw ash content > sodium silicate content.
- For seven-day compressive strength, calcium lime content > sodium silicate content > straw ash content.

Scanning electron microscope analysis

Figure 9 shows the microstructure of two samples viewed

with the scanning electron microscope. There were several activated sediment particles that were not fully involved in the reaction in the 5% straw ash sample. These particles were large, irregular in shape, and embedded or stacked in the generated gel-phase matrix; also, the structure was loose. Due to the low hardness of the material, a stable stress transfer path could not easily form inside of it; therefore, the sample had a low overall uniaxial compressive strength.

In contrast, the gel-phase structure of the compound-doped sample from group SM3 was denser, and the unreacted sediment particles were the least in number and the smallest in

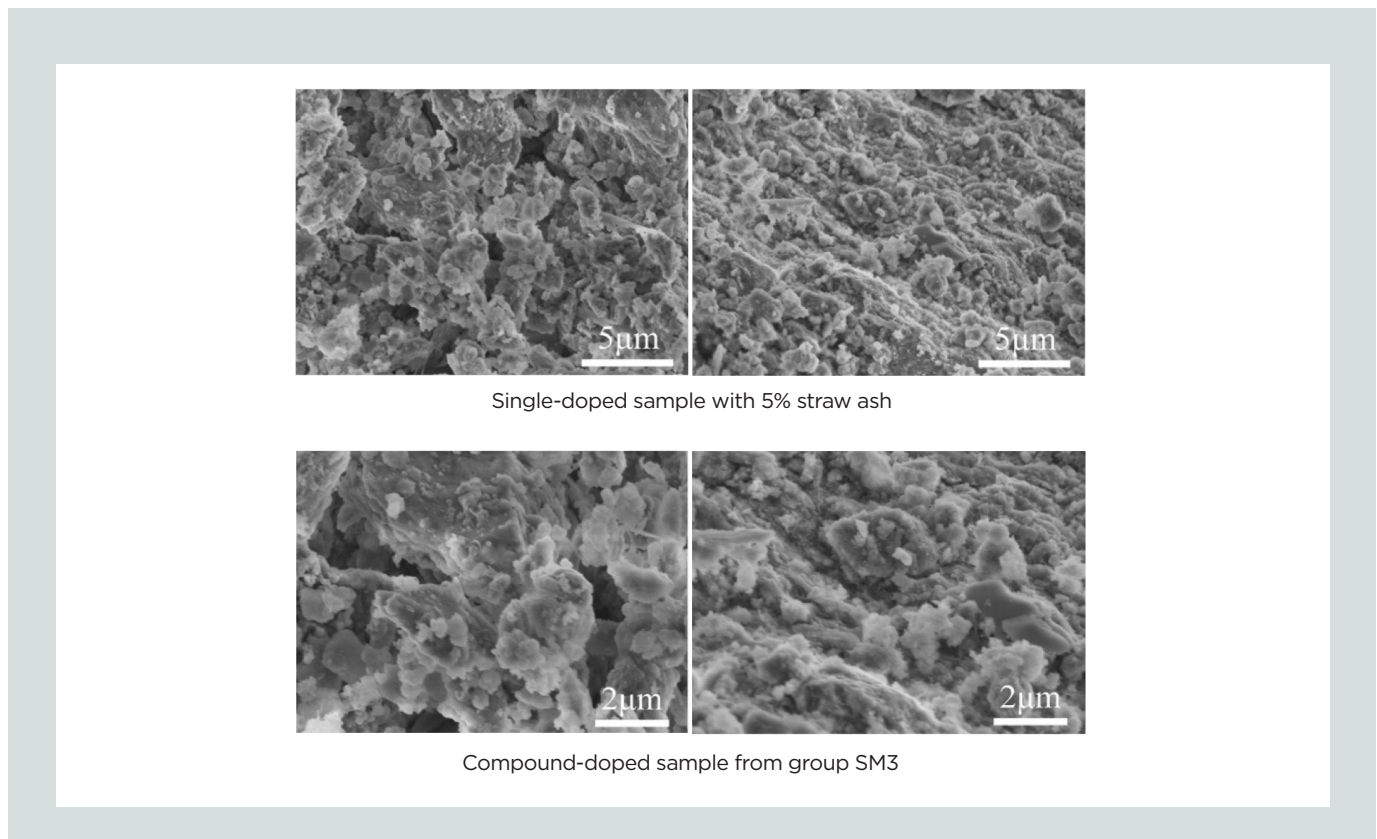


Figure 9. The microstructure of samples viewed with a scanning electron microscope. Note = 1 μm = 0000394 in.

size, thus showing better macroscopic mechanical properties. Notably, the levels of active silicon and active calcium were highest in the SM3 group. Under alkaline conditions, the silicon and calcium could further participate in the reaction to form geopolymer gels with high compressive strength, thereby improving the overall mechanical properties of the sample.

Conclusion

Because scientifically sound, economical, and reliable methods of sediment solidification are needed, the potential use of low-cost straw ash solid waste, calcium lime (as a source of alkaline calcium), and the traditional additive sodium silicate were investigated as curing materials for sediment from Nanh Lake. The following conclusions were drawn based on the experiments conducted:

- The sediment contained large amounts of silicon and aluminum elements, but inactive quartz is the main mineral component. Through the direct sample preparation of the sediment, it was found that the dried sediment sample shrank considerably, cracked easily, and had low compressive strength. Therefore, it would be difficult to directly use or dispose of the sediment without a curing treatment.
- In the single-doped experiments, calcium lime had the greatest solidification effect of the three curing materials. When the calcium lime content was 15%, the maximum seven-day compressive strength of the sample reached 1.31 MPa (190 psi). In the single-doped experiments, the compressive strength of the sample was positively correlated with the percentage of calcium lime or sodium silicate that it contained. The curing effect of straw ash was the least effective. The low alkalinity of straw ash and the introduction of several weak impurities were the main reasons for this material's poor performance.
- The mechanical properties of the samples were improved by using compound-doped materials to solidify the sediment. All samples cured for seven days had compressive strengths greater than 1 MPa (145 psi), and the maximum seven-day compressive strength was 7.18 MPa (1040 psi). This maximum compressive strength was achieved when the straw ash content was 5%, the calcium lime content was 25%, and the sodium silicate content was 25%.
- In addition to providing more suitable alkaline conditions for the solidification reaction of the sediment, the compound-doped materials added large quantities of active silicon and active calcium components, which helped form high-strength geopolymer gel. The microstructure of the solidified sample was more compact than the untreated sediment, and the overall mechanical properties of the sample also significantly improved.

References

1. Zhang, Y., C. Labianca, L. Chen, S.D. Gisi, M. Notarnicola, B. Guo, J. Sun, S. Ding, and L. Wang. 2021. "Sustainable ex-situ Remediation of Contaminated Sediment: A Review." *Environmental Pollution*, no. 287, 117333. <https://doi.org/10.1016/j.envpol.2021.117333>.
2. Lang, L., C. Song, L. Xue, and B. Chen. 2020. "Effectiveness of Waste Steel Slag Powder on the Strength Development and Associated Micro-mechanisms of Cement-stabilized Dredged Sludge." *Construction and Building Materials*, no. 240, 117975. <https://doi.org/10.1016/j.conbuildmat.2019.117975>.
3. Amar, M., M. Benzerzour, J. Kleib, and N. E. Abriak. 2021. "From Dredged Sediment to Supplementary Cementitious Material: Characterization, Treatment, and Reuse." *International Journal of Sediment Research* 36 (1): 92–109. <https://doi.org/10.1016/j.ijsrc.2020.06.002>.
4. Nimwinya, E, W. Arjharn, S. Horpibulsuk, T. Phoonngernkham, and A. Poowancum. 2016. "A Sustainable Calcined Water Treatment Sludge and Rice Husk Ash Geopolymer." *Journal of Cleaner Production*, no. 119, 128–134. <https://doi.org/10.1016/j.jclepro.2016.01.060>.
5. Waijarean, N., S. Asavapisit, and K. Sombatsompop. 2014. "Strength and Microstructure of Water Treatment Residue-Based Geopolymers Containing Heavy Metals." *Construction and Building Materials*, no. 50, 486–491. <https://doi.org/10.1016/j.conbuildmat.2013.08.047>.
6. Waijarean, N., S. Asavapisit, K. Sombatsompop, and K. J. D. MacKenzie. 2014. "The Effect of the Si/Al Ratio on the Properties of Water Treatment Residue (WTR)-Based Geopolymers." *Key Engineering Materials*, no. 608, 289–294. <http://doi.org/10.4028/www.scientific.net/KEM.608.289>.
7. Glukhovskiy, V. D. 1965. "Soil Silicates. Their Properties, Technology and Manufacturing and Fields of Application." Doctoral thesis, Kiev Civil Engineering Institute.
8. Davidovits, J. 1989. "Geopolymers and Geopolymeric Materials." *Journal of Thermal Analysis*, no. 35, 429–441. <https://doi.org/10.1007/BF01904446>.
9. Van Jaarsveld, J. G. S., J. S. J. Van Deventer, and L. Lorenzen. 1997. "The Potential Use of Geopolymeric Materials to Immobilise Toxic Metals: Part I. Theory and Applications." *Minerals Engineering* 10 (7): 659–669. [https://doi.org/10.1016/S0892-6875\(97\)00046-0](https://doi.org/10.1016/S0892-6875(97)00046-0).
10. Wang, P. Z., R. Trettin, and V. Rudert. 2005. "Effect of Fineness and Particle Size Distribution of Granulated Blast-Furnace Slag on the Hydraulic Reactivity in Cement Systems." *Advances in Cement Research* 17 (4):

- 161–167. <https://doi.org/10.1680/adcr.2005.17.4.161>.
11. Almutairi, A. L., B. A. Tayeh, A. Adesina, H. F. Isleem, and A. M. Zeyad. 2021. “Potential Applications of Geopolymer Concrete in Construction: A Review.” *Case Studies in Construction Materials*, no. 15, e00733. <https://doi.org/10.1016/j.cscm.2021.e00733>.
 12. Wu, J., X. Zhen, A. Yang, and Y. Li. 2021. “Experimental Study on the Compressive Strength of Muddy Clay Solidified by the One-part Slag–Fly Ash Based Geopolymer.” *Rock and Soil Mechanics* 42 (3): 647–655. <https://doi.org/10.16285/j.rsm.2020.0918>.
 13. Luo, X., and C. Wang. 2016. “Preparation and Properties of Slag-Based Gelpolymer Porous Materials.” *Journal of the Chinese Ceramic Society* 44 (3): 450–456. <http://doi.org/10.14062/j.issn.0454-5648.2016.03.17>.
 14. Davidovits, J. 1991. “Geopolymers: Inorganic Polymeric New Materials.” *Journal of Thermal Analysis and Calorimetry* 37 (8): 1633–1656. <https://doi.org/10.1007/bf01912193>.
 15. Mikhailova, O., A. Del Campo, P. Rovnanik, J. F. Fernández, and M. Torres-Carrasco. 2019. “In situ Characterization of Main Reaction Products in Alkali-Activated Slag Materials by Confocal Raman Microscopy.” *Cement and Concrete Composites*, no. 99, 32–39. <https://doi.org/10.1016/j.cemconcomp.2019.02.004>.
 16. Nematollahi, B., J. Sanjayan, J. Qiu, and E. H. Yang. 2017. “High Ductile Behavior of a Polyethylene Fiber-Reinforced One-Part Geopolymer Composite: A Micromechanics-Based Investigation.” *Archives of Civil and Mechanical Engineering* 17 (3): 555–563. <https://doi.org/10.1016/j.acme.2016.12.005>.
 17. Luukkonen, T., Z. Abdollahnejad, J. Yliniemi, P. Kinnunen, and M. Illikainen. 2018. “One-Part Alkali-Activated Materials: A Review.” *Cement and Concrete Research*, no. 103, 21–34. <https://doi.org/10.1016/j.cemconres.2017.10.001>.
 18. Su, Y., Luo, B., Luo, Z., Xu, F., Huang, H., Long, Z., and Shen, C. 2023. “Mechanical Characteristics and Solidification Mechanism of Slag/Fly Ash–Based Geopolymer and Cement Solidified Organic Clay: A Comparative Study.” *Journal of Building Engineering*, no. 71, 106459. <https://doi.org/10.1016/j.jobbe.2023.106459>.
 19. Lu, H. F., J. L. Yi, D. He, J. B. Xu, X. X. Kong, and K. Zhang. 2022. “Experimental Study on Preparation of Geological Polymer Grouting Material Based on Dredged Sediment.” *Chinese Journal of Rock Mechanics and Engineering* 41 (12): 2567–2578.
 20. Kong, X., Z. Zhang, Y. Liang, X. Wang, and M. Liu. 2023. “Experimental Study on Solidified Dredged Sediment with MgO and Industrial Waste Residue.” *Construction and Building Materials*, no. 366, 130105. <https://doi.org/10.1016/j.conbuildmat.2022.130105>.
 21. Cong, P., and Y. Cheng. 2021. “Advances in Geopolymer Materials: A Comprehensive Review.” *Journal of Traffic and Transportation Engineering (English Edition)* 8 (3): 283–314. <https://doi.org/10.1016/j.jtte.2021.03.004>.
 22. Palomo, A., M. W. Grutzeck, and M. T. Blanco. 1999. “Alkali-Activated Fly Ashes: A Cement for the Future.” *Cement and Concrete Research* 29 (8): 1323–1329. [https://doi.org/10.1016/S0008-8846\(98\)00243-9](https://doi.org/10.1016/S0008-8846(98)00243-9).
 23. Liu, F., C. Zhu, K. Yang, J. Ni, J. Hai, and S. Gao. 2021. “Effects of Fly Ash and Slag Content on the Solidification of River-Dredged Sludge.” *Marine Georesources and Geotechnology* 39 (1): 65–73. <https://doi.org/10.1080/1064119X.2019.1677827>.
 24. Cheng, X., Y. Chen, G. Chen, and B. Li. 2021. “Characterization and Prediction for the Strength Development of Cement Stabilized Dredged Sediment.” *Marine Georesources and Geotechnology* 39 (9): 1015–1024. <https://doi.org/10.1080/1064119X.2020.1795014>.
 25. Yoobanpot, N., P. Jamsawang, H. Poorahong, P. Jongpradist, and S. Likitlersuang. 2020. “Multiscale Laboratory Investigation of the Mechanical and Microstructural Properties of Dredged Sediments Stabilized with Cement and Fly Ash.” *Engineering Geology*, no. 267, 105491. <https://doi.org/10.1016/j.enggeo.2020.105491>.
 26. Wu, Y., B. Lu, T. Bai, H. Wang, F. Du, Y. Zhang, L. Cai, C. Jiang, and W. Wang. 2019. “Geopolymer, Green Alkali Activated Cementitious Material: Synthesis, Applications and Challenges.” *Construction and Building Materials*, no. 224, 930–949. <https://doi.org/10.1016/j.conbuildmat.2019.07.112>.
 27. Novais, R. M., R. C. Pullar, and J. A. Labrincha. 2020. “Geopolymer Foams: An Overview of Recent Advancements.” *Progress in Materials Science*, no. 109, 100621. <https://doi.org/10.1016/j.pmatsci.2019.100621>.
 28. Temuujin, J. V., A. Van Riessen, and R. Williams. 2009. “Influence of Calcium Compounds on the Mechanical Properties of Fly Ash Geopolymer Pastes.” *Journal of Hazardous Materials*. 167 (1–3): 82–88. <https://doi.org/10.1016/j.jhazmat.2008.12.121>.
 29. Zhang, K., H. Lu, J. Li, and H. Bai. 2022. “Orthogonal Experimental Study on the Factors Affecting the Mechanical Properties of Alkali-Activated Slag Materials.” *Materials* 15 (24): 8795. <https://doi.org/10.3390/ma15248795>.
 30. Wang, X. L., S. X. Yan, and H. Q. Wen. 2013. “Experimental Analysis on Microstructure and Mineral Com-

position of Jurassic Soft Rock in Shajihai Mining Area of Xinjiang.” *Applied Mechanics and Materials*, no. 353–356, 24–27. <https://doi.org/10.4028/www.scientific.net/AMM.353-356.24>.

Mechanisms of Composite Activated Coal Ganguge Geopolymer.” *Construction and Building Materials*, no. 318, 125999. <https://doi.org/10.1016/j.conbuildmat.2021.125999>.

31. Faqir, N. M., R. Shawabkeh, M. Al-Harhi, and H. A. Wahhab. 2019. “Fabrication of Geopolymers from Untreated Kaolin Clay for Construction Purposes.” *Geotechnical and Geological Engineering*, no. 37, 129–137. <https://doi.org/10.1007/s10706-018-0597-5>.
32. Zhang, B., H. Guo, L. Deng, W. Fan, T. Yu, and Q. Wang. 2020. “Undehydrated Kaolinite as Materials for the Preparation of Geopolymer through Phosphoric Acid-Activation.” *Applied Clay Science*, no. 199, 105887. <https://doi.org/10.1016/j.clay.2020.105887>.
33. Alshaaer, M. 2013. “Two-Phase Geopolymerization of Kaolinite-Based Geopolymers.” *Applied Clay Science*, no. 86, 162–168. <https://doi.org/10.1016/j.clay.2013.10.004>.
34. Granizo, M. L., M. T. Blanco-Varela, and S. Martínez-Ramírez. 2007. “Alkali Activation of Metakaolins: Parameters Affecting Mechanical, Structural and Microstructural Properties.” *Journal of Materials Science*, no. 42, 2934–2943. <https://doi.org/10.1007/s10853-006-0565-y>.
35. Shekhawat, P., G. Sharma, and R. M. Singh, R.M. 2020. “Microstructural and Morphological Development of Eggshell Powder and Flyash-Based Geopolymers.” *Construction and Building Materials*, no. 260, 119886. <https://doi.org/10.1016/j.conbuildmat.2020.119886>.
36. Sun, S., J. Lin, L. Fang, R. Ma, Z. Ding, X. Zhang, X. Zhao, and Y. Liu. 2018. “Formulation of Sludge Incineration Residue Based Geopolymer and Stabilization Performance on Potential Toxic Elements.” *Waste Management*, no. 77, 356–363. <https://doi.org/10.1016/j.wasman.2018.04.022>.
37. Wang, S. Y.; Y. Li, and Y. K. Zhang. 2016. “Comparison of Range Analysis and Variance Analysis Methods for Orthogonal Test Results of Concrete.” *Development Guide to Building Materials*, no. 14, 44–48.
38. Zhang, K., J. L. Yi, X. X. Kong, Z. Y. Li, H. F. Lu, Q. Z. Zhang, and B. Feng. 2023. “Preparations of Lake Sediment Geopolymers Using the Alkaline Activation and Their Mechanical Properties.” *Journal of Testing and Evaluation* 51 (5). <https://doi.org/10.1520/JTE20220619>.
39. Chen, C., T. Cheng, W. L. Gong, J. P. Zhai, and M. T. Zhang. 2016. “Analysis of Reaction Factors Under Fly Ash Based Geopolymer System.” *Materials Review*, no. 30, 118–123.
40. Zhao, Y., C. Yang, K. Li, F. Qu, C. Yan, and Z. Wu. 2022. “Toward Understanding the Activation and Hydration

Notation

F	= F -test value, represents the significance of the difference between two or more sample means
$F_{(3,3)0.10}$	= represents the F -critical value where there is at least a 90% probability that two sets of data (both 3 degrees of freedom) have a significant difference
n	= modulus
R_A	= range (difference between the maximum and minimum values of \bar{T}_{Aj})
R_c	= cubic compressive strength of the sample
R_i	= range (difference between the maximum and minimum values of \bar{T}_{ij})
T_{Aj}	= sum of the data of all levels under the factor A
\bar{T}_{Aj}	= mean value (numerically equal to T_{Aj} divided by the levels number)
T_{i1}	= sum of the data of levels 1 under the factor i (A, B or C)
T_{i2}	= sum of the data of levels 2 under the factor i (A, B or C)
T_{i3}	= sum of the data of levels 3 under the factor i (A, B or C)
\bar{T}_{i1}	= mean value (numerically equal to T_{i1} divided by the levels number)
\bar{T}_{i2}	= mean value (numerically equal to T_{i2} divided by the levels number)
\bar{T}_{i3}	= mean value (numerically equal to T_{i3} divided by the levels number)
θ	= the diffraction half angle, the angle between the incident X-ray and the crystal plane that meets the diffraction condition

About the authors



Hongdan Yu is an associate professor for the State Key Laboratory of Geomechanics and Geotechnical Engineering, Institute of Rock and Soil Mechanics at the Chinese Academy of Sciences in Wuhan, Hubei, China.



Kai Zhang is a doctoral student in the School of Civil Engineering and Key Laboratory of Geotechnical and Structural Safety Engineering of Hubei Province at Wuhan University in Wuhan, Hubei, China.



Haifeng Lu is a professor in the School of Civil Engineering and Key Laboratory of Geotechnical and Structural Safety Engineering of Hubei Province at Wuhan University.



Qingzhao Zhang is an associate professor for the School of Civil Engineering and Department of Geotechnical Engineering at Tongji University in Shanghai, China.

Abstract

The disposal of lake sediment is a major problem in dredging and lakeside construction projects. Due to its poor mechanical properties and contamination, sediment is difficult to use directly in resource applications. Previous research has found that alkali-activated reactions can improve the mechanical properties of silicon- and aluminum-rich solid waste. In this study, the basic physical and mechanical properties of dried sediment from a lake in Wuhan, China, were analyzed. Orthogonal tests, compressive strength measurements, and X-ray diffraction spectrum and scanning electron microscope analyses were used to investigate the solidification effects of three types of alkaline materials used alone or in combination with the lake sediment: straw ash, calcium lime, and sodium

silicate. In the single-doped samples, calcium lime had the best curing effect, with a maximum seven-day compressive strength of 1.31 MPa (190 psi). When the compound-doped samples were cured to seven days, the maximum compressive strength was 7.18 MPa (1040 psi). Furthermore, with the compound-doped materials, sediment solidification was aided by suitably alkaline conditions and large quantities of active silicon-calcium components. As a result, the microstructures of the cured compound-doped samples were more compact and their overall mechanical properties were greatly improved.

Keywords

Alkali-activated reaction; compressive strength; lake sediment; orthogonal experiment; sodium silicate; straw ash.

Review policy

This paper was reviewed in accordance with the Precast/Prestressed Concrete Institute's peer-review process. The Precast/Prestressed Concrete Institute is not responsible for statements made by authors of papers in *PCI Journal*. No payment is offered.

Publishing details

This paper appears in *PCI Journal* (ISSN 0887-9672) V. 68, No. 5, September–October 2023, and can be found at <https://doi.org/10.15554/pcij68.5-03>. *PCI Journal* is published bimonthly by the Precast/Prestressed Concrete Institute, 8770 W. Bryn Mawr Ave., Suite 1150, Chicago, IL 60631. Copyright © 2023, Precast/Prestressed Concrete Institute.

Reader comments

Please address any reader comments to *PCI Journal* editor-in-chief Tom Klemens at tklemens@pci.org or Precast/Prestressed Concrete Institute, c/o *PCI Journal*, 8770 W. Bryn Mawr Ave., Suite 1150, Chicago, IL 60631. 